Supplemental Material

Highly excited exciton-polariton condensates

Tomoyuki Horikiri,[1, 2, 3, 4, 5,] Tim Byrnes,[6, 7, 8, 9, 10] Natsuko Ishida,[5, 4] Yasuhiro Matsuo,[4] Yutaka Shikano,[11, 12, 13, 14] Andreas Loffler,[15] Sven Hofling,[15, 16, 2] Alfred Forchel,[15] and Yoshihisa Yamamoto[2, 3, 17]

[1]*Yokohama National University, Tokiwadai 79-5, Hodogaya-ku, Yokohaa, Kanagawa 240-8501, Japan*
[2]*National Institute of Informatics, Hitotsubashi 2-1-2, Chiyoda-ku, Tokyo 101-8430, Japan*
[3]*E. L. Ginzton Laboratory, Stanford university, Stanford, California 94305, USA*
[4]*The University of Tokyo, 7-3-1 Hongo, Bunkyo-ku, Tokyo 113-8656, Japan*
[5]*Center for Emergent Matter Science, RIKEN, 2-1 Hirosawa, Wakoshi, Saitama 351-0198, Japan*
[6]*State Key Laboratory of Precision Spectroscopy, School of Physical and Material Sciences, East China Normal University, Shanghai 200062, China*
[7]*NYU-ECNU Institute of Physics at NYU Shanghai, 3663 Zhongshan Road North, Shanghai 200062, China*
[8]*National Institute of Informatics, 2-1-2 Hitotsubashi, Chiyoda-ku, Tokyo 101-8430, Japan*
[9]*New York University Shanghai, 1555 Century Ave, Pudong, Shanghai 200122, China*
[10]*Department of Physics, New York University, New York, NY 10003, USA*
[11]*Research Center of Integrative Molecular Systems, Institute for Molecular Science, 38 Nishigo-Naka, Myodaiji, Okazaki 444-8585, Japan*
[12]*Institute for Quantum Studies, Chapman University, 1 University Dr., Orange, California 92866, USA.*
[13]*Materials and Structures Laboratory, Tokyo Institute of Technology, 4259 Nagatsuta, Midori, Yokohama 226-8503, Japan.*
[14]*Research Center for Advanced Science and Technology (RCAST), The University of Tokyo, 4-6-1 Komaba, Meguro-ku, Tokyo, 153-8904, Japan*
[15]*Technische Physik, Universit• at W• urzburg, Am Hubland, D-97074 W• urzburg, Germany*
[16]*SUPA, Schoold of Physics and Astronomy, University of St Andrews, KY16 9SS, United Kingdom.*
[17]*ImPACT Program, Japan Science and Technology Agency,7 Gobancho, Chiyoda-ku, Tokyo 102-0076, Japan.*

1. Sample: transition to weak coupling at high temperature

12 GaAs quantum wells (QW) (divided into 3 groups with 4 QWs each) are embedded at antinodes of the microcavity consisting of AlAs/AlGaAs distributed Bragg reflectors. The normal mode splitting at k=0 was 14 meV. The detuning at k=0 between microcavity photon and QW exciton energies was chosen to be zero at a temperature of 8 K. The negative branch of the excitation spectrum was only observable in small detuning parameter regime close to zero.

In Figure S1, temperature dependence of normal modes is seen below threshold. With temperature increase, the red-shift rate of the QW exciton energy is larger than that of the cavity photon energy. Therefore, the cavity photon energy becomes above the band gap energy at very high temperatures. The normal modes at 200 K are clearly separated more than 20 meV showing weak coupling. Thus, the sample shows the strong coupling condition at low temperatures (e.g. 8 K) and weak coupling condition at high temperatures (e.g. 200 K). At high temperatures, where the thermal energy k_BT exceeds the exciton binding energy, the device is expected to operate as a vertical cavity surface emitting laser (VCSEL). This is confirmed by an effective mass measurement which we estimate to be about $\sim 3\times10^{-35}$ kg, approximately one half of LP mass for zero detuning and equal to a bare cavity photon mass (See Figure S3).

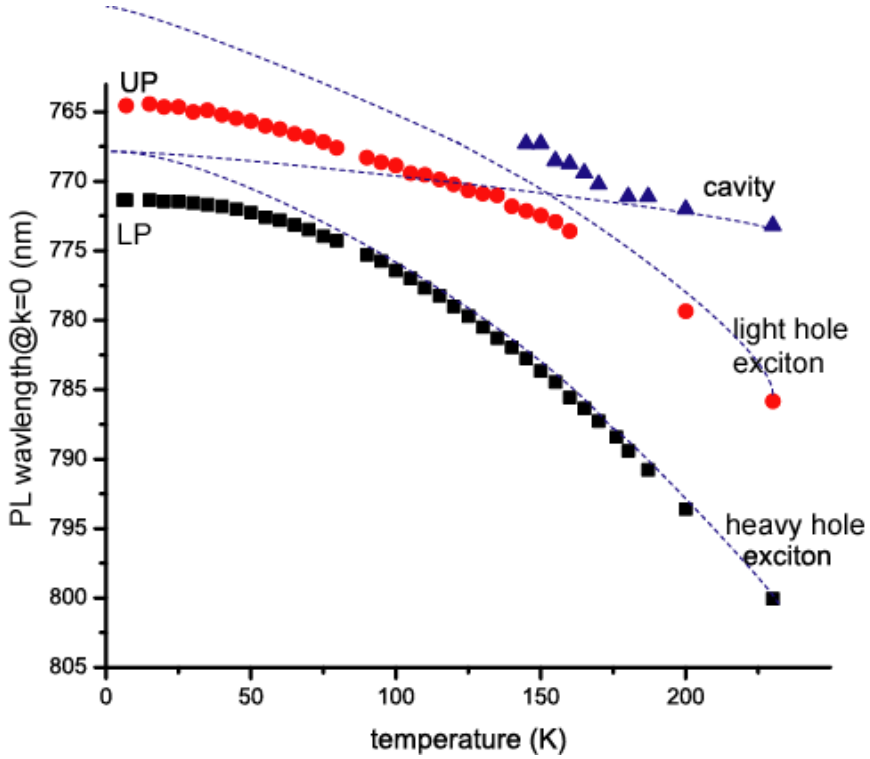

Figure S1 | Temperature dependence of normal PL energies of GaAs 12 QW microcavity structure. Normal mode at low temperatures (LP and UP) at k=0 shows red-shift as temperature scanning which leads to normal modes' transition into heavy-hole (HH) exciton, light-hole (LH) exciton and cavity photon. Dotted curves are for eye-guiding. Both LP and UP red-shift with increasing temperature, and they gradually turn into the cavity photon, HH exciton, and LH exciton. At temperatures around 150-180K, strong coupling between the cavity photon and LH exciton occurs, which is eventually lost around 200 K.

2. Time-resolved dispersion measurement by a streak camera

We carried out time-resolved spectroscopy of dispersion relations [27] with a streak camera attached to a monochromator to only examine the time yielding maximum excitation density. To avoid a reduced time-resolution, the lens in front of the monochromator had a 100 mm focal length introducing a small numerical aperture that caused a small beam spot size at the grating, and hence the temporal dispersion induced by the grating could be reduced to around 10 ps in this study.

One acquisition corresponded to one wavenumber with a finite width (Δk), which was determined by the vertical slit positioned at the entrance of the streak camera. We used a

slit width of 20 μm in the present study. One measurement corresponding to a certain k having a width Δk' corresponds to a vertical band in the Fig. 2c and 2d. Δk'(>Δk) is a serve as a visual guide since Δk is small. The ratio of the expanded width is five times (Δk'=5Δk.). The k-plane was scanned by moving the lens in front of the monochromator. A spectrum with the maximum PL intensity corresponding to the maximum excitation density was extracted from each measurement data. The dispersion in Fig. 2 was obtained using the combined spectra acquired at various values of inplane-momentum. The data are composed of 25 points of different. Therefore, the constructed dispersion from finite k points have gaps due to the small number of measurement points. The data around k=0 are dense due to the smaller scanning steps.

The validity of the measurement can be shown by the comparison between time-integrated data and time-resolved data in Figure S2, where normal LP dispersions below threshold are shown. For the time-resolved dispersion measurement, the measurement must be done by scanning k with moving an imaging lens in front of the monochromator attached before the streak camera. A detection width of Δk determined by a vertical slit width of the streak camera determines the resolution of the dispersion measurement. We scanned more than 20 points for obtaining dispersion curves in Fig. 2 in main text and the right hand side of Figure S2. The actual Δk at each k is much narrower than the displayed (about 1/7 (for Fig. S2) and 1/5 (for Fig.3 in main text) of the displayed Δk are the actual detection width at each k), however, we used the present bin for eye-friendly display. The white curve of the time-resolved data in Fig. S2 is the fitting result by a quadratic curve near k=0 which give the effective mass of LP and the result is compared with the data of high excitation density in Fig. 2 in the main text where the positive and negative branches curvatures are shown to be the same as the normal LP branch.

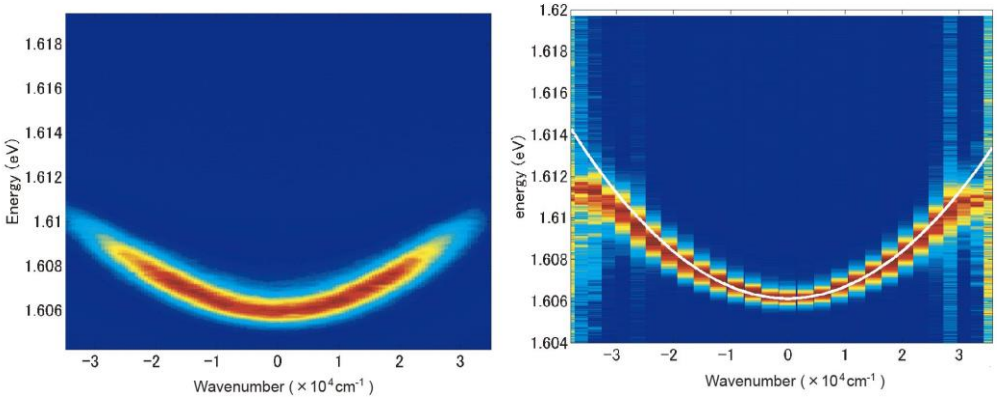

Figure S2 | Time-integrated (left) and time-resolved (right) dispersion data below condensation threshold. Each figure's color scale means the PL intensity. However, in the case of the time-resolved data (right panel), the PL intensity is normalized at each k. Therefore, the PL at large k seems to be as bright as the PL at k=0, though actually the PL is much weaker as in the case of the time-integrated case (left panel).

In the final part of this section, we show a typical time-evolution of PL at one in-plane momentum in Fig. S3. We extracted a time giving maximum PL at each momentum to obtain Fig.2c and 2d in main text.

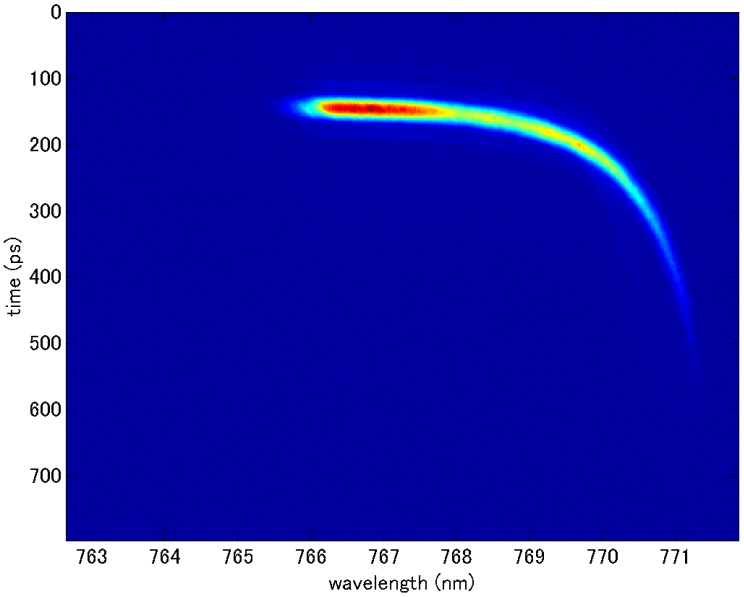

Figure S3 | Time-evolution of PL at one in-plane momentum at a pump power where we could observe a negative branch.

3. Dispersion characteristics at high temperature weak coupling regime

Here we show dispersion characteristics for high temperature (200 K) and several excitation densities, where we can clearly see VCSEL type laser emission. A narrowing of the PL spectrum occurs and its intensity increases nonlinearly at threshold (Fig. S4b and Fig. 3 in main text). Unlike the LP condensate, a slight red shift is observed (instead of the self-interaction induced blue shift), which is due to the red shift of the cavity photon energy with increasing temperature. Even at very high excitation density (Fig. S4c) the linewidth is much narrower than 8 K case, which suggests pure photon lasing is occurring. No negative dispersion was observed at this high temperature, which also confirms the lack of polariton-polariton interaction.

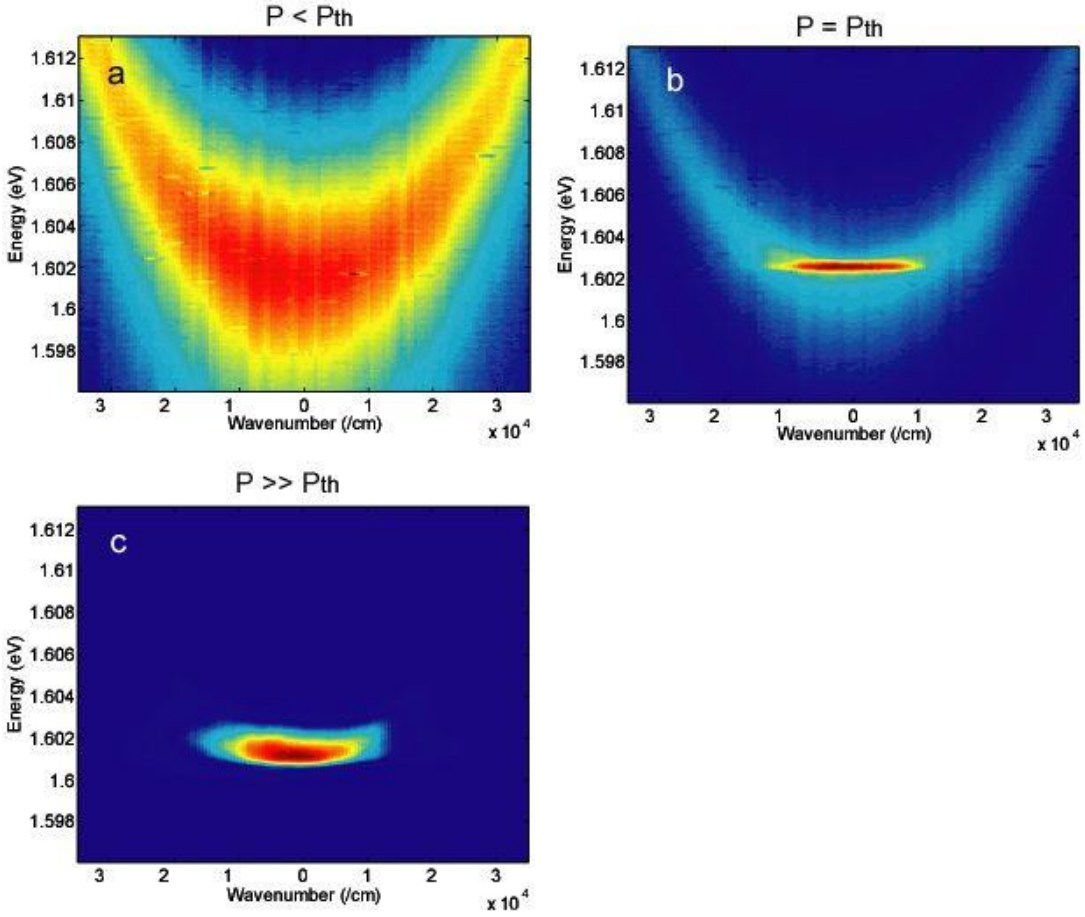

Figure S4 | Transition to a standard photon laser at high temperature (200 K). **a-c,** Energy-momentum dispersions at various pump powers as shown at 200K. **a**. Below threshold, **b**. At threshold, **c**. Far above threshold. Above threshold, photon lasing is exhibited, as can be seen from the sharp PL emission at the cavity photon energy.